Improving the fabrication of all-polythiophene supercapacitors[1]

Margarita Sánchez-Jiménez,[a] Francesc Estrany[a,b] and Carlos Alemán[b,c]

[a] *Departament d'Enginyeria Química, Escola Universitària d'Enginyeria Tècnica Industrial de Barcelona, Universitat Politècnica de Catalunya, Comte d'Urgell 187, 08036 Barcelona, Spain*
[b] *Center for Research in Nano-Engineering, Universitat Politècnica de Catalunya, Campus Sud, Edifici C', C/Pasqual i Vila s/n, Barcelona E-08028, Spain*
[c] *Departament d'Enginyeria Química, E. T. S. d'Enginyers Industrials, Universitat Politècnica de Catalunya, Diagonal 647, 08028, Barcelona, Spain*
[*] francesc.estrany@upc.edu and carlos.aleman@upc.edu

Received

Abstract. The influence of the preparation method in the properties of poly(3,4-ethylenedioxythiophene) (PEDOT) electrodes used to manufacture organic energy storage devices, as for example supercapacitors, have been examined by considering a reduction of both monomer and supporting electrolyte concentrations during the anodic polymerization reaction. Thus, the excellent electrochemical properties of PEDOT films prepared using quiescent solutions have been preserved by applying controlled agitation to the polymerization process, even though the concentration of monomer and supporting electrolyte were reduced 5 and 2 times, respectively. For example, the charge stored for reversible exchange in a redox process, the electrochemical stability and the current productivity of films achieved using quiescent solutions have been preserved using a dynamic reaction medium in which the concentrations of monomer and supporting electrolyte are several times lower. The excellent properties of PEDOT electrodes prepared using optimized dynamic conditions have also been proved by constructing a symmetric supercapacitor. This energy storage device, which has been used as power source for a LED bulb, is rechargeable and exhibits higher charge-discharge capacities than supercapacitors prepared with electrodes derived from quiescent solutions. In addition of bring an efficacious procedure for preparing cost-effective PEDOT films with excellent properties, the proposed dynamic conditions reduce the environmental hazards of depleted reaction media.

Keywords: Conductivity; Charge transport; Conjugated polymers; Electrochemistry; Organic supercapacitors

---

[1] This work was supported by MINECO/FEDER (MAT2015-69367-R) and by the "ICREA Academia" (Generalitat de Catalunya) for excellence in research to C.A.

INTRODUCTION

Nowadays, with the increasing use of portable electronic devices, electric vehicles and other electronic products, research has been focused on energy storage. Within this context, supercapacitors based on Faradaic electron-transfer processes are considered a promising kind of energy storage devices owing to their high power capability and long cycle life [1,2]. Thus, many recent efforts have been oriented to improve the performance of supercapacitors from materials and devices perspectives [3-5]. Electroactive conducting polymers (ECPs) are typical examples of supercapacitor materials because they can be readily charged and discharged by converting between different redox states [6]. This conversion process is associated with the dopant ions diffusion into / out of the ECP matrix to keep the electroneutrality. Thus, in order to achieve high power at high charge/discharge rate, the fast conversion rate of the redox states, which is governed by dopant ion diffusion, has to be preserved.

Among commercially available ECPs, poly(3,4-ethylenedioxythiophene) (PEDOT) is the most important due to its high electrical conductivity (even higher than $5\cdot10^3$ S/cm), good transparency, excellent electrochemical and thermal stabilities, fast doping-dedoping processes and biocompatibility [7-14]. PEDOT can be synthesized by electrochemical polymerization using an active supporting electrolyte or by oxidative chemical polymerization to obtain aqueous dispersions stabilized by a water-soluble poly(styrene sulfonate) [15-17]. In last years, PEDOT and its derivatives have been widely applied in the energy field, as for example to fabricate the cathode and anode in all-organic supercapacitors [18,19], electrochemical microactuators [20], and catalysts for polymer electrolyte fuel cells [21,22]. Furthermore, in a very recent study, solid-state organic electrochemical supercapacitors have been fabricated combining PEDOT electrodes, a biohydrogel as electrolyte system, and polyaniline fibers as redox additive [23].

On the other hand, we recently examined the effects of controlled dynamical conditions (*i.e.* stirring the generation solution with a magnetic bar) in the anodic polymerization process and in the properties of PEDOT [24]. For this purpose, PEDOT films were prepared in presence and absence of solution agitation (*i.e.* stirred and quiescent solutions, respectively) using a minimal concentration of monomer. Thus, the increase in the transport rate produced by controlled agitation, which accelerates the electropolymerization, allowed us to optimize the yielding by reducing significantly the concentration of monomer in the generation medium. It should be remarked that until such study the information reported in the literature about the influence of dynamical stirring in the polymerization and properties of ECPs was very scarce [25-27]. This was an amazing feature since we found that controlled agitation improves significantly the flow of monomer at the electrode surface and affects the organization of polymer chains in the resulting films [24]. More specifically, our results indicated that the increase in transport rate of reactants slightly favors the generation of more polymer weight at equal charge consumed. Consequently, the thickness of the materials prepared under stirring increases considerably with respect to those obtained from quiescent solutions. Moreover, the porosity of PEDOT films also increases upon agitation, facilitating the dopant ions diffusion into / out of the ECP matrix upon reduction and oxidation processes.

In this work we go a step further improving the preparation methods of PEDOT electrodes for organic supercapacitors and batteries by considering, besides a decrease in the concentration of monomer, a reduction of the concentration of supporting electrolyte during the anodic polymerization reaction. For this purpose, we will investigate the electrochemical and topographic properties of electrodes derived from stirred and quiescent solutions with different supporting electrolyte concentrations. Furthermore, the impact of this modification in the performance of organic supercapacitors has been also evaluated. Results provide not only an effective procedure for preparing PEDOT electrodes for energy applications, reducing considerably their cost by minimizing the concentration of both monomer and electrolyte without any detriment in the capabilities of the energy storage devices, but also to reduce the environmental hazards of depleted reaction media.

EXPERIMENTAL

Anodic polymerization. PEDOT films were prepared by chronoamperometry (CA) under a constant potential of 1.40 V [16] with a PGSTAT101 AUTOLAB potentiostat-galvanostat connected to a PC computer and controlled through the NOVA 1.6 software. All electrochemical experiments were conducted in a three electrode one-compartment cell under nitrogen atmosphere (99.995% in purity) at room temperature. The cell was filled with 50 mL of an acetonitrile solution of the corresponding monomer and $LiClO_4$ as supporting electrolyte. The polymerization time was 100 or 300 s in all cases.

The working and counter electrodes consisted of steel AISI 316 sheets of area 1×1 cm^2. In order to avoid interferences during the electrochemical analyses, the working and counter electrodes were cleaned with acetone and dried in an air-flow before each trial. The reference electrode was an Ag|AgCl electrode containing a KCl saturated aqueous solution (E^0 = 0.222 V *vs.* standard hydrogen electrode at 25°C). All the potentials reported in this work are referred to the latter electrode.

PEDOT films were prepared in presence and absence of solution agitation, hereafter denoted as dynamic and static conditions, respectively. A magnetic bar and a stirrer SBS were used for the dynamical conditions. The rotation speed was fixed at 400 rpm, which was found to provide the most stable and highest value of the current density [24].

The electrochemical activity and stability (electroactivity and electrostability, respectively) of the prepared PEDOT films were determined by cyclic voltammetry (CV). The initial and final potential was -0.50 V, whereas the reversal potential was 1.60 V. All measurements were performed at room temperature using a scan rate of 100 mV/s. The electroactivity, which refers to the charge storage ability, was defined as the maximum voltammetric stored charge per surface unit (Q, in C/cm^2) in the second oxidation-reduction cycle. The electrostability was evaluated as the variation of Q with consecutive oxidation-reduction cycles.

Atomic force microscopy (AFM). Topographic AFM images were obtained with a Dimension 3100 Nanoman AFM and Multimode from Veeco using a Nanoscope IV controller under ambient conditions in tapping mode. AFM measurements were performed on various parts of the films, which produced reproducible images similar to those displayed in this work. The root-mean-square roughness (Rq), arithmetic average roughness (Ra) and the maximum roughness value (Rmax) were determined using the statistics application and tools of the NanoScope Analysis software version 1.20 (Bruker). The scan window sizes were 5×5 µm^2.

RESULTS AND DISCUSSION

Influence of the supporting electrolyte concentration using quiescent solutions

Figure 1 represents the electroactivity and electrostability of PEDOT films prepared under static conditions considering different monomer (10 and 2 mM EDOT) and supporting electrolyte (50, 100 and 200 mM $LiClO_4$) concentrations. As it can be seen, the ability to store charge of films derived from quiescent solutions clearly increases with the monomer concentration, even though for each EDOT concentration both the role exerted by the supporting electrolyte concentration is also relevant. For films produced using 10 mM EDOT, the electroactivity and electrostability were very similar for 100 and 200 mM $LiClO_4$, decreasing around 30% for 50 mM $LiClO_4$. In contrast, both electrochemical properties decrease with increasing $LiClO_4$ concentration for ECP films obtained using 2 mM EDOT (Figure 1 inset).

These results clearly indicate that the electrochemical properties of ECP films obtained in absence of stirring depend on the concentrations of supporting electrolyte and, specially, of monomer in the generation medium. Regarding to the supporting electrolyte, electrochemical properties do not improve after surpass a given threshold concentration (*optimum* value). Indeed, such properties become even worse for the case with the lowest monomer concentration, which is the most appropriated when dynamic conditions are used (see below).

Influence of the supporting electrolyte concentration using dynamic conditions

Figure 2a displays the electroactivity and electrostability of PEDOT films obtained using dynamic conditions and a polymerization time of 100 s. The concentration of monomer in the reaction medium was 2 mM in all cases, which was identified as the optimum value in our previous study [24], while the following LiClO4 concentrations were considered: 100, 50 and 20 mM. As it can be seen, the electroactivity increases with the concentration of supporting electrolyte, even though the charged stored in

PEDOT films prepared using 100 and 50 mM $LiClO_4$ is relatively similar (*i.e.* 46 and 34 mC/cm^2, respectively). On the other hand, the loss of electroactivity is similar (*i.e.* ~30% after 25 redox cycles) for all PEDOT films prepared using dynamic conditions, independently of the electrolyte concentration.

The electrochemical properties of the films obtained using dynamic conditions are very similar, or even better, than those obtained using static conditions and a higher concentration of monomer and/or supporting electrolyte (Figure 2a). The most striking example refers to films prepared using a 2mM EDOT concentration: those derived from 50 mM $LiClO_4$ quiescent solutions are 30% and 65% less electroactive than films obtained using 20 and 50 mM $LiClO_4$ stirred solutions, respectively.

In order to further improve the electrochemical properties of PEDOT films prepared using dynamic conditions, the polymerization time was enlarged from 100 to 300 s to increase their thickness. Electroactivity and electrostability results, which have been extended to 100 redox cycles, are summarized Figure 2b. Comparison with results displayed in Figure 2a indicates that charge stored by PEDOT films prepared using dynamic conditions and 2 mM EDOT concentrations increased significantly with the polymerization time for both 20 and 50 mM $LiClO_4$ concentrations. More specifically, the electroactivity increment is 180% for both electrolyte concentrations. In contrast, the electroactivity of PEDOT films using static conditions increases ~80% only when the polymerization time is enlarged from 100 and 300 s. Indeed, the electroactivity of PEDOT is significantly higher for films prepared under dynamic conditions than under static ones (Figure 2b). In terms of electrostability the benefit is apparently lower, even though after 100 redox cycles the electroactivity of PEDOT is 180% and 520% higher for films derived from stirred solutions than from quiescent solutions for 20 and 50 mM $LiClO_4$ concentrations, respectively.

Current productivity

The influence of the concentration of electrolyte on the kinetics for the oxidation-polymerization of EDOT was studied by generating films under fixed experimental conditions (*i.e.* constant potential of 1.40 V, 2 mM monomer concentration, 50 or 20 mM $LiClO_4$, and stirred or quiescent solutions) and considering different polymerization times. Graphical representation of the film weight (W_{ox}), which was reproducible for polymerization times lower than 500 s, against the charge (Q_{pol}) consumed in the polymerization process, which was derived from the registered chronoamperograms, is displayed in Figure 3. Linear correlations were obtained for all dynamic and static conditions (*i.e.* R^2 comprised between 0.9553 and 0.9940), reflecting that these are Faradaic processes. However, this consistency is more pronounced for films prepared under dynamic conditions, as prove the fact that $R^2 > 0.97$ for both $LiClO_4$ concentrations.

The slope of the adjusted equation, $Q_{pol}= a\cdot W_{ox}$, corresponds to the current productivity, which is expressed as milligrams of PEDOT electrogenerated per Coulomb (C) of charge consumed during the anodic polymerization. It is worth noting that, for the two $LiClO_4$ concentrations, the current productivity is higher for films derived from stirred solutions than from quiescent ones. That difference is higher than 20% for films prepared using 50 mM $LiClO_4$. Moreover, for the two dynamic conditions displayed in Figure 3, the mass–charge ratio is close to the standard value of 0.8 mg/C obtained using 10 mM EDOT and 100 mM $LiClO_4$ [16].

Surface topography

Representative 3D topographic AFM images of PEDOT films prepared using 2 mM EDOT, a polymerization time of 100 s and different concentrations of $LiClO_4$ (20, 50 and 100 mM) under both dynamic and static conditions, are displayed in Figure 4.

The surface topography of films prepared using dynamic conditions exhibit rounded and relatively high peaks, independently of the $LiClO_4$ concentration. The latter essentially affects to the abundance and height of the peaks, as is clearly reflected by the Rq, Ra and Rmax values listed in Table 1. More specifically, the surfaces of films obtained using the two lower concentrations of supporting electrolyte are dominated by deep valleys, which separate rounded peaks grouped in small clusters. When the concentration of $LiClO_4$ increases from 20 to 50 mM, the depth of the valley decreases, which explains the reduction of the roughness. Thus, the enlargement of electrolyte concentration induces the incorporation of EDOT monomers to shorter polymer chains, leveling the surface of the film. However, this effect is moderate, as is shown by the fact that the different values of roughness decreases by only 10-20%. The influence of the supporting electrolyte is slightly more pronounced when its concentration increases from 50 to 100 mM since the height of the peaks and, specially, the size of the clusters increases considerably. Consequently, Rmax increases 47% while the increment of both Rq and Ra is around 30%. In this case the addition of electrolyte induces the elimination of some valleys giving place to apparition of new rounded and very high peaks.

In spite of the discussed differences, it should be remarked that the three films obtained using dynamic conditions exhibit similar topographical trends. This has been attributed to the fact that the diffusion of electrolyte ions is considerable enhanced by the agitation and, therefore, the concentration of perchlorate ions at the polymer / medium interphase is in all cases significantly higher than expected for the corresponding quiescent solutions (see below). Consequently, the impact of the concentration of supporting electrolyte on the surface topography is moderate when polymer films are obtained under dynamic conditions.

In opposition, topographic features of films derived from quiescent solutions greatly depend on the $LiClO_4$ concentration (Figure 4). In films derived from the lowest supporting electrolyte concentration (20 mM), polymer chains tend to organize forming a dense distribution of relatively sharp, narrow and low peaks. Consequently, measured roughness values are ~65% lower than those of films obtained using stirred solutions with the same $LiClO_4$ concentration. Although the width and height of the clustered peaks in films from quiescent solutions increases with the $LiClO_4$ concentration, which is due the grouping of the sharp and narrow peaks observed for 20 mM $LiClO_4$, these parameters as well as their abundance are considerably lower than those observed for films obtained using dynamic conditions. More specifically, the size and abundance of valleys increases and decreases, respectively, with increasing concentration of electrolyte, while the height and size of the clusters decreases and increases, respectively. Consequently, the structure becomes less uneven and more closed with increasing $LiClO_4$ concentration. These topographies is less favorable to the exchange of ions between the polymeric matrix and the medium during redox processes than the ones observed for films obtained using dynamic conditions.

Comparison of all-PEDOT supercapacitors prepared using static and dynamic conditions

On the basis of the above discussed results, symmetric supercapacitors were fabricated by combining an oxidized PEDOT electrode (anode) with a reduced PEDOT electrode (cathode). PEDOT electrodes were prepared using stirred acetonitrile solution with 2 mM EDOT and 50 mM $LiClO_4$ and quiescent solution with 10 mM EDOT and

100 mM $LiClO_4$. Oxidized and reduced PEDOT electrodes were obtained by applying a current of +1.0 mA during 280 s (doping process) and a current of -1.0 mA during 190 s (dedoping process), respectively. The half-reactions upon discharge of supercapacitors fabricated using PEDOT electrodes derived from dynamic and static conditions, hereafter denoted SC/D and SC/S, respectively, are:

Anode: $$\mathrm{PEDOT}^{x+}\,(\mathrm{ClO}_4^-)_x + x\mathrm{e}^- \rightarrow \mathrm{PEDOT}^0 + x\mathrm{ClO}_4^-$$

Cathode: $$\mathrm{PEDOT}^0 + x\mathrm{ClO}_4^- \rightarrow \mathrm{PEDOT}^{x+}\,(\mathrm{ClO}_4^-)_x + x\mathrm{e}^-$$

For each supercapacitor two cells were assembled in series (Figure 5a), reaching a voltage window of ~3.8 V and ~2.2 V for SC/D and SC/S, respectively. The assembled systems were connected to a red LED bulb (Figure 5a), which required a voltage of ~1.5 V to power on. PEDOT supercapacitors fabricated with electrodes obtained using static and dynamic conditions allowed us to maintain the power of the LED bulb during intervals of time of ~ 1 min and ~2.5 min, respectively, a discharge cutoff potential of 1.5 V being reached after that time. Recharging of the supercapacitors was carried out by coupling a power supply of 12 V and a resistance of 10 kΩ. Such two elements were retired after complete the recharge, which took ~250 and ~65 s for SC/D and SC/S, respectively. These recharge-power processes were repeated by more than 10 times without detriment in the performance of the supercapacitors.

The discharge curves of the supercapacitors are provided in Figure 5b, which represents the voltage dropping of charged devices against the discharge time. A resistance of 1 kΩ was used for the discharge process, measures being performed every 5 s. The values displayed in Figure 5b correspond to the average of three independent experiments for each supercapacitor. The voltage of SC/D is higher than that of the SC/S during the first ~2 min, after such time the drop is practically the same for the two devices. Finally, the stability of the SC/D devices was proved by applying ten consecutive charge-discharge processes, in which the LED bulb was kept powered during the charging processes. Figure 5c, which shows the curves for the first and tenth charge-discharge process, reflects that the performance of the device remains practically unaltered.

CONCLUSIONS

Results obtained in this work clearly indicates that PEDOT films prepared using agitated reaction media, in which the concentrations of both the monomer and the supporting electrolyte are considerably lower than those used in typical quiescent solutions, exhibit excellent electrochemical properties. Interestingly, the topography of PEDOT films achieved using dynamic conditions is relatively independent of the supporting electrolyte concentration because the diffusional effects provoked by the agitation ensures a relative high concentration of ions at the polymer / medium interphase. Fabrication of all-PEDOT supercapacitors by assembling two cells made with films prepared using dynamic conditions evidence that such topography favors significantly the mobility of ions. Thus, the performance (*i.e.* reached voltage window, powering of a LED bulb, discharge rate and re-chargeability) of supercapacitors fabricated using dynamic conditions is higher than that of devices obtained using quiescent solutions with much higher monomer and supporting electrolyte concentrations. This investigation is relevant not only for improvement of the PEDOT electrodes but also for the environmental impact of their fabrication. Thus, reduction of the reactants concentrations provokes a favorable effect in the environmental hazards of depleted reaction media.

Table 1. Root-mean-squared roughness (Rq), arithmetic average roughness (Ra) and the maximum roughness value (Rmax) of PEDOT films obtained by CA at a constant potential of 1.40 V using a 2mM EDOT acetonitrile solution, a polymerization time of 100 s and different $LiClO_4$ concentrations (20, 50 and 100 mM) and agitation conditions (dynamic and static).

[$LiClO_4$]	**Stirred / Quiescent**	**Rq (nm)**	**Ra (nm)**	**Rmax (nm)**
20 mM	Dynamic	280	225	1603
	Static	93.4	74.1	641
50 mM	Dynamic	251	203	1388
	Static	263	211	1545
100 mM	Dynamic	325	259	2036
	Static	202	157	1272

CAPTIONS TO FIGURES

Figure 1. Electroactivity (maximum voltammetric charge stored for reversible exchange in the second redox cycle) and electrostability (variation of the maximum charge voltammetric stored for reversible exchange with the number of redox cycles) of PEDOT films prepared in absence of solution agitation (static conditions) using different monomer (EDOT) and supporting electrolyte ($LiClO_4$) concentrations. In all cases, electroactivity measurements are expressed as voltammetric charge per surface unit (Q).

Figure 2. Electroactivity (maximum voltammetric charge stored for reversible exchange in the second redox cycle) and electrostability (variation of the maximum charge voltammetric stored for reversible exchange with the number of redox cycles) of PEDOT films prepared in presence of solution agitation (dynamic conditions) using a 2 mM EDOT concentration and different supporting electrolyte ($LiClO_4$) concentrations. Results for selected PEDOT films prepared using static conditions have been included for comparison. The polymerization time was 100 s in all cases. (b) Electroactivity and electrostability of PEDOT films prepared in absence and presence of solution agitation (static and dynamic conditions) using a 2 mM EDOT concentration and different supporting electrolyte ($LiClO_4$) concentrations. The polymerization time was 300 s in all cases. In both (a) and (b), electroactivity measurements are expressed as voltammetric stored charge per surface unit (Q).

Figure 3. Variation of the weight of PEDOT films (W_{ox}) deposited onto steel from a 2 mM EDOT solution in acetonitrile with 50 or 20 mM $LiClO_4$ at a constant potential of 1.40 V under static and dynamic conditions against the polymerization charge (Q_{pol}) consumed. Temperature: 25 ºC. The current productivity (mg of PEDOT per Coulomb

of charge consumed during the electropolymerization) for each condition corresponds to the slope of the linear equation displayed for each plot.

Figure 4. 3D AFM topographic images of PEDOT films prepared using dynamic (left) and static (right) conditions. The concentration of EDOT monomer in the reaction medium was kept at 2 mM EDOT in all cases, while the concentration of supporting electrolyte was varied as is indicated.

Figure 5. (a) Photographs of the all-PEDOT SC/D device constructed using PEDOT electrodes that were obtained using agitated acetonitrile solutions with 2 mM EDOT and 50 mM $LiClO_4$. The SC/D device was used to power the LED bulb for more than ~2.5 min (a video is available upon request to the authors). (b) Discharge profile for the SC/D and SC/S devices using a resistance of 1 kΩ. (c) First and tenth charge-discharge cycles for the SC/D device (the LED bulb was kept powered during the whole charge-discharge process).

REFERENCES

1. K. Naoi, S. Ishimoto, J. Miyamoto, and W. Naoi, Energy Environ. Sci., 5, 9393 (2012).
2. S.A. Sherrill, P. Banerjee, G.W. Rubloff, and S.B. , Phys. Chem. Chem. Phys., 13, 20714 (2011).
3. K. Fic, G. Lota, M. Meller, and E. Frackowiak, Energy Environ. Sci., 5, 5842 (2012).
4. J. Shen, A. Liu, Y. Tu, G. Foo, C. Yeo, M.B. Chan-Park, R. Jiang, and Y. Chen, Energy Environ. Sci., 4, 4220 (2011).
5. C. Peng, S. Zhang, D. Jewell, and G.Z. Chen, Prog. Nat. Sci., 18, 777 (2008).
6. H.-K. Song, and G.T.R. Palmore, Adv. Mater., 18, 1764 (2006).
7. H. Okuzaki, H. Suzuki, and T. Ito, J. Phys. Chem. B, 113, 11378 (2009).
8. R.H. Karlsson, A. Herland, M. Hamedi, J. A. Wigenius, A. Åslund, X. Liu, M. Fahlman, O. Inganäs, and P. Konradsson, Chem. Mater., 21, 1815 (2009).
9. M.V. Fabretto, D.R. Evans, M. Mueller, K. Zuber, P. Hojati-Talemi, R.D. Short, G.G. Wallace, and P.J. Murphy, Chem. Mater., 24, 3998 (2012).
10. M. Mueller, M. Fabretto, D. Evans, P. Hojati-Talemi, C. Gruber, and P. Murphy, Polymer, 53, 2146 (2012).
11. B.L. Groenendaal, G. Zotti, P.H. Aubert, S.M. Waybright, and J.R. Reynolds, Adv. Mater., 15, 855 (2003).
12. L.J. Del Valle, F. Estrany, E. Armelin, R. Oliver, and C. Alemán, Macromol. Biosci., 8, 1144 (2008).
13. W. Loevenich, Polym. Sci. Ser. C, 56, 135 (2014).

14. M. N. Gueye, A. Carella, N. Massonnet, E. Yvenou, S. Brenet, J. Faure-Vincent, S. Pouget, F. Rieutord, H. Okuno, A. Benaya, R. Demadrille, and J.-P. Simonato, Chem. Mater., 28, 3462 (2016).
15. J. Liu, B. Wei, J.D. Sloppy, L. Ouyang, C. Ni, and D.C. Martin, ACS Macro Lett., 4, 897 (2015).
16. C. Ocampo, R. Oliver, E. Armelin, C. Alemán, and F. Estrany, J. Polym. Res., 13, 193 (2006).
17. M. Lefebvre, Z. Qi, D. Rana, and P.G. Pickup, Chem. Mater., 11, 262 (1999).
18. Y. Xuan, M. Sandberg, M. Berggren, and X. Crispin, Org. Electron., 13, 632 (2012).
19. D. Aradilla, F. Estrany, F. Casellas, J. I. Iribarren, and C. Alemán, Org. Electron., 15, 40 (2014).
20. S. Taccola, F. Greco, B. Mazzolai, V. Mattoli, and E.W.H. Jager, J. Micromech. Microeng., 23, 117004 (2013).
21. J.A. Vigil, T.N. Lambert and K. Eldred, ACS Appl. Mater. Interfaces, 7, 22745 (2015).
22. K.K. Tintula, A. Jalajakshi, A.K. Sahu, S. Pitchumani, P. Sridhar, and A.K. Shukla, Fuel Cells, 13, 158 (2013).
23. M.M. Pérez-Madrigal, F. Estrany, E. Armelin, D. Díaz-Díaz, and C. Alemán, J. Mater. Chem. A, 4, 1792 (2016).
24. M. Sánchez-Jiménez, C. Alemán, and F. Estrany, Polym. Eng. Sci., 54, 2121 (2014).
25. E. Brillas, J. Carrasco, R. Oliver, F. Estrany, J. Vilar, and J.M. Morlans, Electrochim. Acta, 45, 4049 (2000).

26. F. Estrany, R. Oliver, E. Garcia, E. Gualba, P.L. Cabot, and E. Brillas, Collect. Czech. Chem. Commun., 68, 1326 (2003).

27. J. Tietje-Girault, C. Ponce de León, and F.C. Walsh, Surf. Coat. Technol., 201, 6025 (2007).

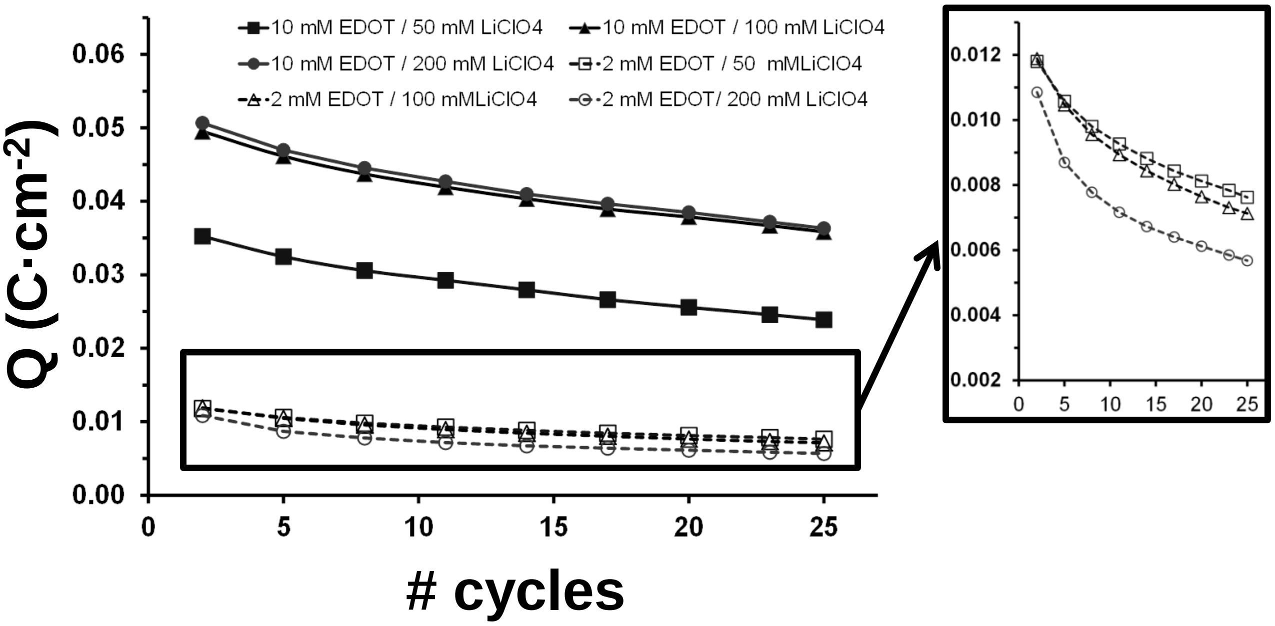
10 mM EDOT / 50 mM LiClO4
10 mM EDOT / 100 mM LiClO4
10 mM EDOT / 200 mM LiClO4
2 mM EDOT / 50 mMLiClO4
2 mM EDOT / 100 mMLiClO4
2 mM EDOT/ 200 mM LiClO4
Q (C·cm-2)
0.06
0.05
0.04
0.03
0.02
0.01
0.00
0
5
10
15
20
25
cycles
0.012
0.010
0.008
0.006
0.004
0.002
0
5
10
15
20
25

Figure 1

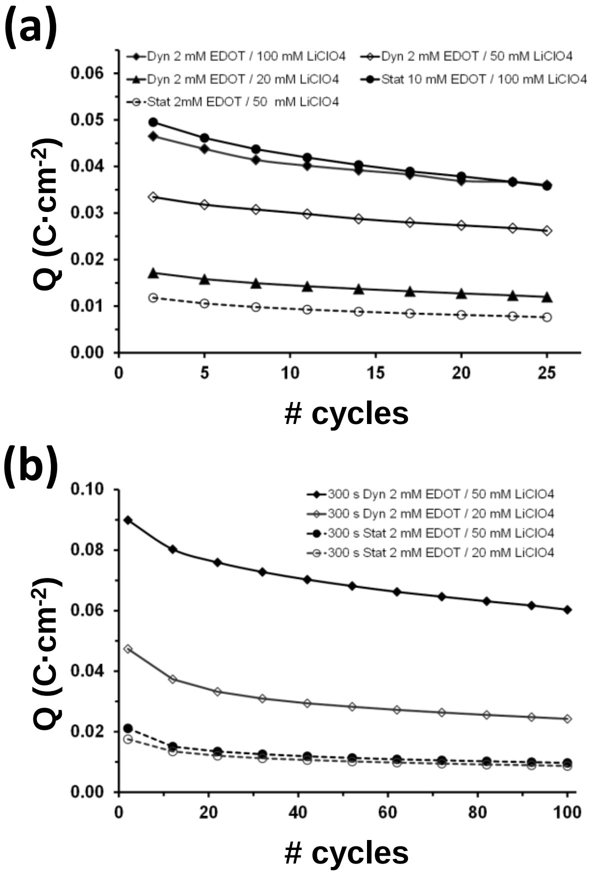
(a)
Dyn 2 mM EDOT / 100 mM LiClO4
Dyn 2 mM EDOT / 50 mM LiClO4
Dyn 2 mM EDOT / 20 mM LiClO4
Stat 10 mM EDOT / 100 mM LiClO4
Stat 2mM EDOT / 50 mM LiClO4
Q (C·cm^{-2})
0.06
0.05
0.04
0.03
0.02
0.01
0.00
0
5
10
15
20
25
cycles
(b)
300 s Dyn 2 mM EDOT / 50 mM LiClO4
300 s Dyn 2 mM EDOT / 20 mM LiClO4
300 s Stat 2 mM EDOT / 50 mM LiClO4
300 s Stat 2 mM EDOT / 20 mM LiClO4
Q (C·cm^{-2})
0.10
0.08
0.06
0.04
0.02
0.00
0
20
40
60
80
100
cycles

Figure 2

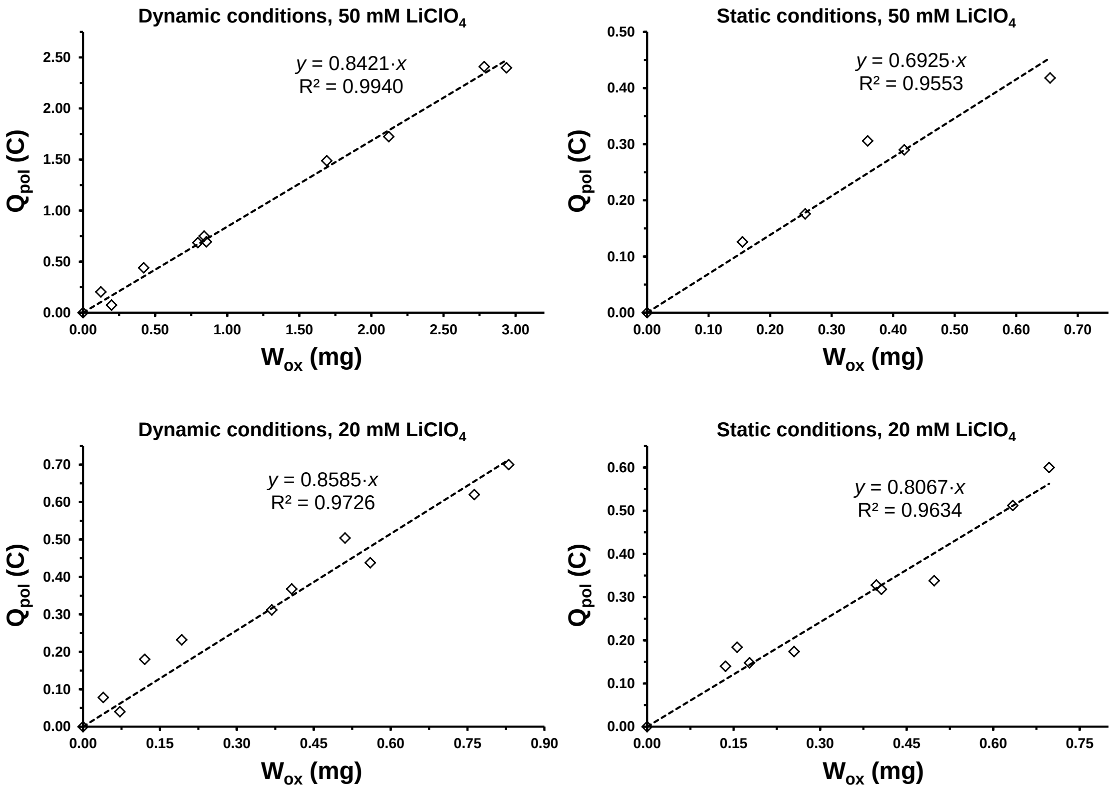
Dynamic conditions, 50 mM $LiClO_4$

Static conditions, 50 mM $LiClO_4$

Dynamic conditions, 20 mM $LiClO_4$

Static conditions, 20 mM $LiClO_4$

Figure 3

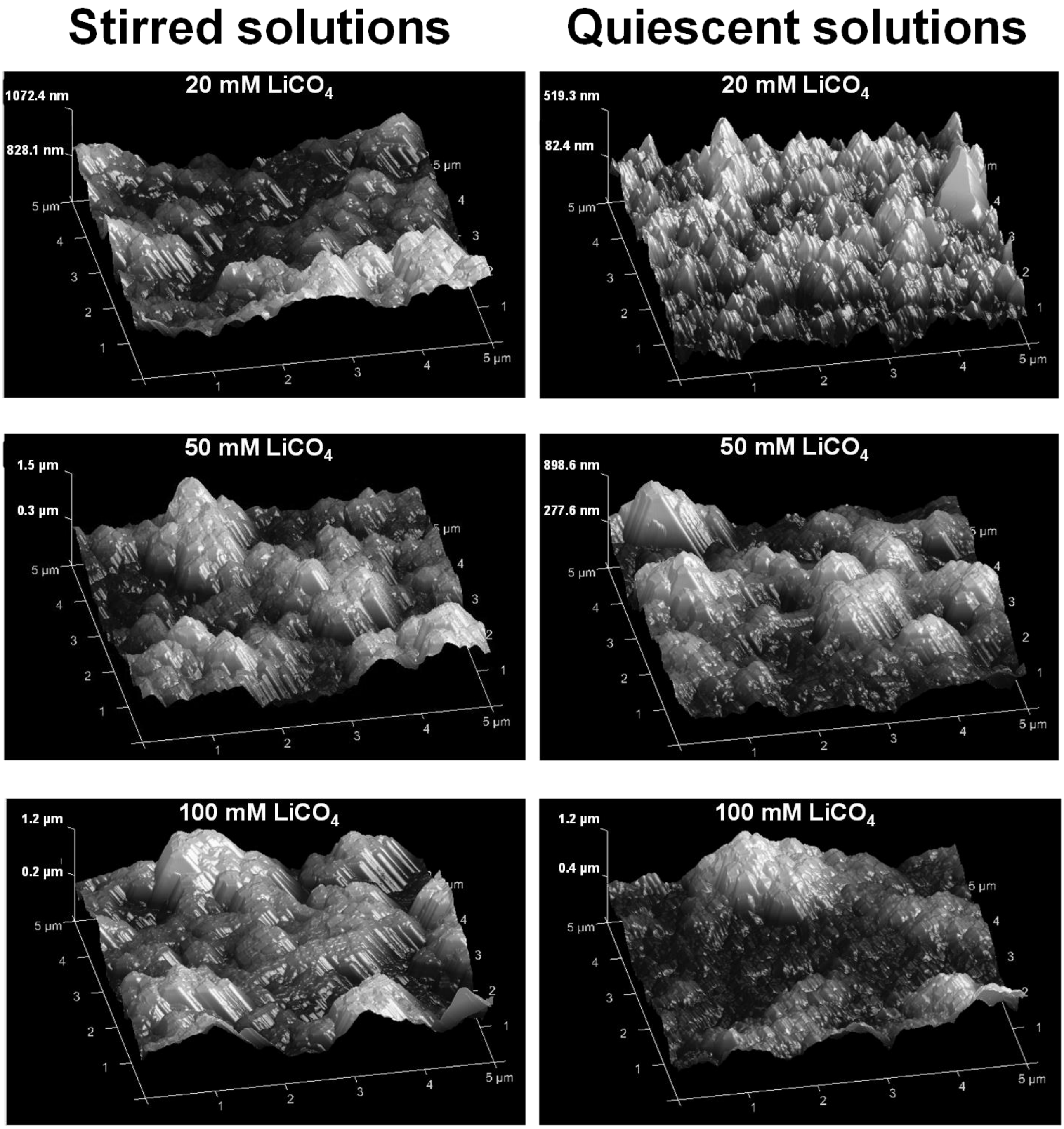
Stirred solutions
Quiescent solutions
20 mM LiCO$_4$
1072.4 nm
828.1 nm
519.3 nm
82.4 nm
50 mM LiCO$_4$
1.5 µm
0.3 µm
898.6 nm
277.6 nm
100 mM LiCO$_4$
1.2 µm
0.2 µm
1.2 µm
0.4 µm
1
2
3
4
5 µm

Figure 4

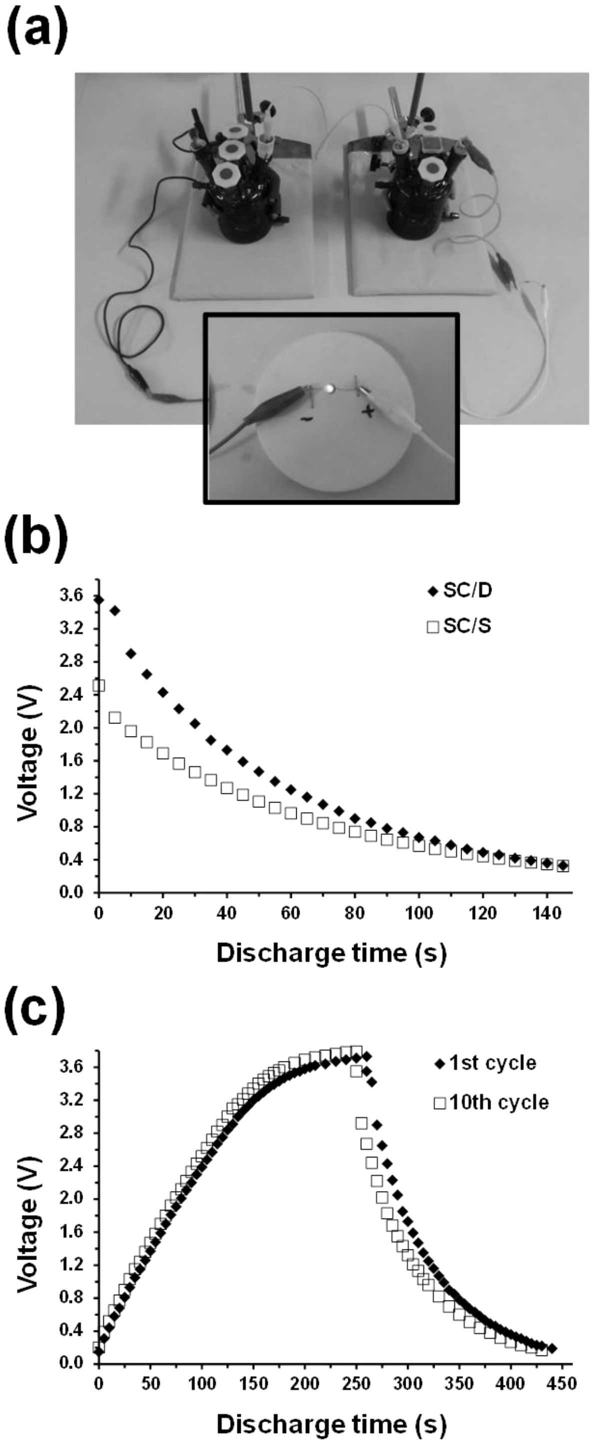
(a)
+
-
(b)
◆ SC/D
□ SC/S
Voltage (V)
3.6
3.2
2.8
2.4
2.0
1.6
1.2
0.8
0.4
0.0
0
20
40
60
80
100
120
140
Discharge time (s)
(c)
◆ 1st cycle
□ 10th cycle
Voltage (V)
3.6
3.2
2.8
2.4
2.0
1.6
1.2
0.8
0.4
0.0
0
50
100
150
200
250
300
350
400
450
Discharge time (s)

Figure 5